



Original Article

***Nod2* Deficiency Leads to a Specific and Transmissible Mucosa-associated Microbial Dysbiosis Which Is Independent of the Mucosal Barrier Defect**

Ziad Al Nabhani,^{a,b,c,d} Patricia Lepage,^{c,d} Pascal Mauny,^e
Nicolas Montcuquet,^{f,g} Maryline Roy,^{a,b} Karine Le Roux,^{c,d}
Monique Dussillant,^{a,b} Dominique Berrebi,^{h,i} Jean-Pierre Hugot,^{a,b,j}
Frédéric Barreau^{a,b,k}

^aLaboratoire d'excellence Inflammex, Université Paris-Diderot Sorbonne Paris-Cité, France ^bINSERM, UMR 1149, F-75018 Paris, France ^cINRA, MICALIS-UMR1319, Jouy-en-Josas, France ^dAgroParisTech, MICALIS-UMR1319, Jouy-en-Josas, France ^eCNRS, TAAM, Orléans, France ^fINSERM, UMR 989, F-75015 Paris, France ^gUniversité Paris Descartes – Sorbonne Paris Cité, Institut IMAGINE, Paris, France ^hServices d'anatomie et de cytologie pathologiques, Hôpital Robert Debré, Université Paris-Diderot Sorbonne Paris-Cité, Paris, France ⁱUMR996, Cytokines, chimiokines et immunopathologie, Clamart, France ^jServices des maladies digestives et respiratoires de l'enfant et service d'anatomie pathologique, Hôpital Robert Debré, Paris, France. ^kInstitut de Recherche en Santé Digestive, Université de Toulouse, Toulouse, France

Corresponding author: Dr. Frédéric Barreau, IRSD, Hopital Purpan - Place du Docteur Baylac CS 60039, 31024 Toulouse cedex 3, France Tel: +33 5 62 74 45 45; Fax: +33 5 62 74 45 38; email: frederick.barreau@inserm.fr

Abstract

Background and Aims: Crohn's disease [CD] is a complex disorder characterised by an inappropriate immune response, impaired barrier function and microbial dysbiosis. Mutations in nucleotide oligomerisation domain 2 [*NOD2*] are CD risk factors. Increase of intestinal permeability, CD4⁺ T cell infiltration, and bacterial dysbiosis are also seen in *Nod2*-knockout [*Nod2*^{KO}] mice. However, the specificity and relationship between these *Nod2*-associated abnormalities remain largely unexplored.

Methods: Wild-type [WT], *Nod1*-knockout [*Nod1*^{KO}] and *Nod2*^{KO} mice were analysed in parallel. Microbial composition was defined by 454-pyrosequencing of bacterial 16S rRNA genes. Mucin and antimicrobial peptide expression was assessed by RT-PCR. Cell populations from Peyer's patches were determined by flow cytometry. Ussing chambers were used to measure intestinal permeability and bacterial translocation. Finally, to explore the impact of colonisation with mother's microbiota at birth, analyses were also performed in *Nod2*^{KO} and WT mice born from WT surrogate mothers after embryo transfer.

Results: *Nod2*^{KO} mice exhibited colonic bacterial dysbiosis different from WT and *Nod1*^{KO} mice. Altered expression of antimicrobial peptides and mucins in ileum and colon was associated with the microbial composition. Bacterial composition of *Nod2*^{KO} and WT mice obtained by embryo transfer was similar to that observed in *Nod2*^{KO} mice, arguing for a dominant effect of *Nod2*^{KO}-associated dysbiosis. In contrast, increased levels of CD4⁺ T cells and gut barrier defects across Peyer's patches were specific to *Nod2* deficiency and independent of Microbial dysbiosis.

Conclusions: *Nod2* deficiency is associated with a specific dominant dysbiosis which does not drive mucosal tissue and immune alterations.

Key Words: Crohn's disease; gut barrier dysfunction; intestinal microbiota; Nod-like

1. Introduction

The gastrointestinal mucosa is the body's main interface between the external environment and the internal milieu. In healthy people, the three compartments of the digestive mucosa which include immune system, epithelial barrier and commensal bacteria, are in homeostatic steady state. Failure of intestinal homeostasis results in numerous human diseases including inflammatory,¹ metabolic,^{2,3} infectious,⁴ and neurological disorders.⁵ Most of these are complex multifactorial diseases, involving genetic and environmental factors, such as Crohn's disease [CD].⁶

NOD2 [nucleotide-binding oligomerization domain containing 2] mutations are associated with an increased risk to develop CD.⁷ *NOD2*, expressed in both haematopoietic and non-haematopoietic cellular compartments, is a cytosolic sensor that recognises muramyl-dipeptide [MDP] present in the cell wall of Gram-positive and -negative bacteria.⁸ Binding of MDP to *NOD2* results in expression of inflammatory cytokines, chemokines, antimicrobial molecules, and induction of adaptive immune responses.⁹

Patients with CD harbour altered intestinal microbial communities characterised by an increase in Bacteroidetes and Proteobacteria and a decrease of Firmicutes.¹⁰ The effect of *Nod2* on the gut microbiota was observed in both *Nod2* knockout [*Nod2*^{KO}] mice and CD patients with *NOD2* mutations.^{11,12,13,14,15,16} However, co-housing *Nod2*^{KO} and control mice suppressed or minimised differences in gut microbial composition.^{17,18} Coprophagia may have an impact on microbial composition and possibly shades differences in the microbiota caused by genetic defects. Microbial composition may also be affected by host proteins such as mucins and antimicrobial peptides.¹⁹ Indeed, *Nod2*^{KO} mice display reduced expression of Paneth cell-derived antimicrobial cryptidins.²⁰ However, another study did not show a decrease in cryptidin expression in *Nod2*^{KO} mice.¹⁸ Moreover, *Nod2*^{KO} mice were also shown to display defects in mucus production by goblet cells, as well as abnormalities in the epithelium.¹² Thus, altered host gene expression can modify commensal bacterial communities. In this study, we sought to resolve the mechanisms underlying an association between intestinal microbiota and host gene expression.

The gut-associated lymphoid tissue [GALT] consists of isolated and aggregated lymphoid follicles forming Peyer's patches [PPs]. PPs are induction sites of immune tolerance or defence against pathogens, which result from a complex interplay between resident immune cells and follicle-associated epithelium.²¹ This cross-talk is regulated by pathogen recognition receptors, especially *Nod2*.⁴ *Nod2* signalling in response to intestinal bacteria results in regulation of T cell responses as well as of PP permeability.^{22,23} However, the link of bacterial dysbiosis and *Nod2* deficiency to the alteration of immune cell populations and dysfunction of gut permeability remains unknown.

Here we show that *Nod2* deficiency induces a specific and dominant bacterial dysbiosis in the colon. Modification of microbial composition is also associated with an abnormal expression of both antimicrobial peptides and mucins. Finally, we show that the abnormalities in GALT function are specific to *Nod2* deficiency and independent of the composition of gut microbiota.

2. Material and Methods

2.1. Mice

C57BL/6 wild-type, *Nod1*^{KO24} and *Nod2*^{KO22} mice were housed in specific pathogen-free conditions and monitored every 6 months in accordance with the full set of FELASA high-standard recommendations. Housing and experiments were conducted according to institutional animal healthcare guidelines and were approved by the local ethical committee for animal experimentation [Comité Régional d'Ethique en matière d'Expérimentation Animale no. 4, Paris, France].

Embryo transfers were used to limit the impact of environmental factors on composition of the gut microbiota. For this, 20 embryos from WT or *Nod2*^{KO} mice were mixed and transferred into the uterus of pseudopregnant C57BL/6 female mice. WT or *Nod2*^{KO} pups were separated from their mother at weaning and were subsequently co-housed [maintained in the same cage].

All mice were euthanised at 10 weeks of age. Samples from each mouse included mucosal scrapings of 2 cm from terminal ileum and colon for bacterial analysis as well as tissue from ileum and colon to assess host gene expression.

2.2. Quantitative real-time polymerase chain reaction for gene expression analysis

RNA was extracted from ileum and colon tissues using the NucleoSpin RNA II Kit [Macherey-Nagel, France], converted to cDNA using random hexanucleotides, and then used for real-time polymerase chain reaction [RT-PCR] as previously described.²⁵ Quantitative [q]PCR was performed with QuantiTect SYBR Green PCR Kit [Applied, France] using specific sense and antisense primers [see Table S1, available as Supplementary data at ECCO-JCC online]. After amplification, threshold cycles [Ct] were determined to obtain expression values in form of 2^{-ΔΔCt}. The investigated genes included: RegIII-γ [regenerating islet-derived protein 3-gamma] and RegIII-β [regenerating islet-derived protein 3-beta], bactericidal C-type lectins that specifically target Gram-positive bacteria; Muc2, Muc3, Muc4, and Muc13 are protein constituents of mucus lining the intestinal epithelium; TFF3 [intestinal trefoil factor] is largely restricted to goblet cells of the small and large intestine; Fc-γ binding protein [Fc-γ Bp] is expressed in the granular mucus of goblet cells and contributes to cross-linkage and stabilisation of mucin networks in the inner mucus layer²⁶; and Ang4 [angiogenin 4] which has been identified as a Paneth cell-derived antimicrobial peptide which is important for epithelial host defence against gut-dwelling bacteria in the small intestine.²⁷ Lysozyme [pLys] and secretory phospholipase A2 [sPLA2] are secreted by Paneth cells.²⁸ MMP-7 [matrix metalloproteinase-7] regulates the activity of cryptidins in the intestinal mucosa. Cryptidin [α-defensin] includes cryptidin-1, cryptidin-5, and cryptidin-6; cryptidin-related sequence 1C [CRS1C] and pan-cryptidin are common to all cryptidins except cryptidin-4 and cryptidin-5, both of which are secreted by Paneth cells against Gram-positive and -negative bacteria.^{28,29}

2.3. Microbial DNA extraction and 454 pyrosequencing of gut microbiota

Total DNA was extracted from 70 mucosal scrapings as previously described,^{14,30} using both physical and chemical lysis. DNA

concentrations were determined spectrophotometrically using a Nanodrop [Thermo Scientific]. Microbial composition was assessed by 454 pyrosequencing [GSFLX technology] targeting the V3-V4 region of the bacterial 16S rRNA gene [V3fwd: 5'TACGGRAGGCAGCAG3', V4rev: 5'GGACTACCAGGGTATCTAAT3']. Sequences were trimmed to remove barcodes and PCR primers and were subsequently selected for a minimal sequence length of 300 pb, a minimal base quality threshold of 27, and a maximum homopolymer length of 6. Sequences were further clustered into OTUs [Operational Taxonomic Units or phylotypes] at 97% of identity using QIIME³¹ and cd-hit.³² OTU representative sequences were assigned to the different taxonomic levels [from phylum to genus and first relative bacterial species] using RDP Seqmatch [RDP database, release 11, update 1].³³ Relative abundance of each OTU and other taxonomic levels [from phylum to genus] was calculated for each sample in order to take into account different sampling levels across multiple individuals. After trimming, numbers of sequences clustered within each OTU [or other taxonomic levels] were converted to a fraction representing the relative contribution of each feature to the corresponding individual. For analysis of microbiota, all statistics were performed using R [ade4 package]. For heatmap representations, log₁₀-transformation was applied on the relative abundance data matrix. This allowed visualisation of similarities or differences between samples that affect members of the community, that may account for less than 1% of the relative abundance in a sample. Hierarchical clustering was computed based on Pearson's correlation coefficient using the Ward distance. Spearman rank correlation was applied to analyse associations between variations in antimicrobial peptide and mucin expression levels and bacterial genera composition. Principal components analysis [PCA] was computed based on bacterial taxonomic composition and statistically assessed by Monte Carlo rank test. Robustness of each clustering result was assessed using Monte Carlo rank test [B = 10 000 repetitions, $p < 0.05$].³⁴ Mann-Whitney testing was applied to assess statistical significance of differences in bacterial compositions between samples.

2.4. Paracellular permeability and bacterial translocation

Biopsies from PPs, ileum, or colon were mounted in Ussing chambers, exposing 0.196 cm² of tissue surface to 1.5 ml of circulating oxygenated Ringer solution at 37°C. Paracellular permeability was assessed by measuring the mucosal-to-serosal flux of 4 kDa FITC-dextran²² [Sigma, France]. Bacterial translocation across PPs was studied using chemically killed fluorescein-conjugated *Escherichia coli* K12 at a final concentration of 10⁷ CFU/ml in the mucosal reservoir, as previously shown.³⁵

2.5. Peyer's patch analysis

PPs were dissected from mice and washed with cold phosphate-buffered saline [PBS]. Cell suspensions from PPs were prepared by manually extracting the cells using a previously validated protocol.²³ Cells were centrifuged, washed in PBS, and erythrocytes were lysed by addition of Gey's solution. Cells from PPs were re-suspended in 2 ml of PBS and counted. For flow cytometric analysis, cell suspensions [10⁵ cells] were incubated with PE-, FITC-, APC, or PerCP-conjugated monoclonal antibodies [mAbs] against mouse CD3, CD4, CD8, CD11c and CD19 [BD Biosciences]. Labelled cells were analysed with a BD-LSR II cytometer and CELLQuest software [BD Biosciences] as previously described.³⁶

2.6. Histological analysis

Samples of ileum and colon for wild-type and *Nod2*^{KO} mice [$n = 4$ /group] were fixed in formalin and routinely processed. Orientation of the crypts by haematoxylin and eosin and thus periodic acid-Schiff staining and lysozyme (monoclonal antibody [ABD serotec], dilution 1/200 on paraffin sections using Bond Max Leica automate) immunohistochemistry were performed, highlighting goblet and Paneth cells, respectively. We assessed the number of goblet and Paneth cells for 50 ileal and colonic crypts.

2.7. Statistical analysis

Multigroup comparisons were performed via one-way analysis of variance [ANOVA] followed by a Bonferroni multiple comparison test including a p -value correction according to the number of tests performed. Gaussian distribution was tested by Kolmogorov-Smirnov testing. Statistical analyses were performed using GraphPad Prism 5.00 [GraphPad Software]. A value of $p < 0.05$ was considered statistically significant. All p -values were considered two-sided.

3. Results

3.1. *Nod2* deficiency leads to specific mucosa-associated microbial dysbiosis

To investigate the impact of *Nod2* deficiency on the mucosa-associated microbial composition, mucosal scrapings from terminal ileum and distal colon were examined in wild-type [WT], *Nod1*^{KO} [control of specificity toward *Nod2*], and *Nod2*^{KO} mice. *Nod2* deficiency led to a higher proportion of Bacteroidetes and a lower representation of Firmicutes in colon but not in ileum [Figure 1A and Supplementary Figure 1A, available as Supplementary data at ECCO-JCC online]. *Nod2*^{KO} mice exhibited an increase in the relative number of bacteria assigned to the Porphyromonadaceae family and a concomitant decrease in bacteria from Lachnospiraceae in colon compared with WT mice [Figure 1B]. In contrast, the proportion of Lactobacillaceae and Deferribacteraceae families was increased in *Nod1*^{KO} mice [Figure 1B]. A hierarchical clustering dendrogram based on colonic bacterial genera distribution allowed discrimination between the three mouse strains [Figure 1C]. Principal components analysis [PCA] at the genus level confirmed that bacterial communities in *Nod2*^{KO} mice differ from the microbial composition in *Nod1*^{KO} and WT control mice, highlighting that the genetic defects contributed to changes in the microbial composition [Figure 1C, Monte-Carlo test $p = 10^{-5}$].

In particular, the colonic mucosa from *Nod2*^{KO} mice displayed higher proportions of bacteria assigned to the genus *Barnesiella* and unclassified Porphyromonadaceae and lower levels of *Clostridium IV* as compared with WT mice [Supplementary Figure 1B]. When compared with *Nod1*^{KO} mice, *Nod2*^{KO} mice had higher levels of *Parabacteroides* but were deprived of the *Turicibacter* genus in ileum and colon, highlighting bacterial dysbiosis specific to *Nod2* deficiency [Supplementary Figure 1B and 1C]. In addition, Gram-negative bacterium cL10-2b-4 [*Barnesiella* genus] and Gram-negative bacterium cTPY-13 [unclassified Porphyromonadaceae] were the main species detected in the colon [Supplementary Figure 2A, available as Supplementary data at ECCO-JCC online]. In terminal ileum, the percentage of sequences similar to segmented filamentous bacteria X77814 [SFB] varied between all groups of mice [Supplementary Figure 1C and 2B]. However, these results did not allow a reliable conclusion in favour of specific *Nod2*-associated ileal dysbiosis.

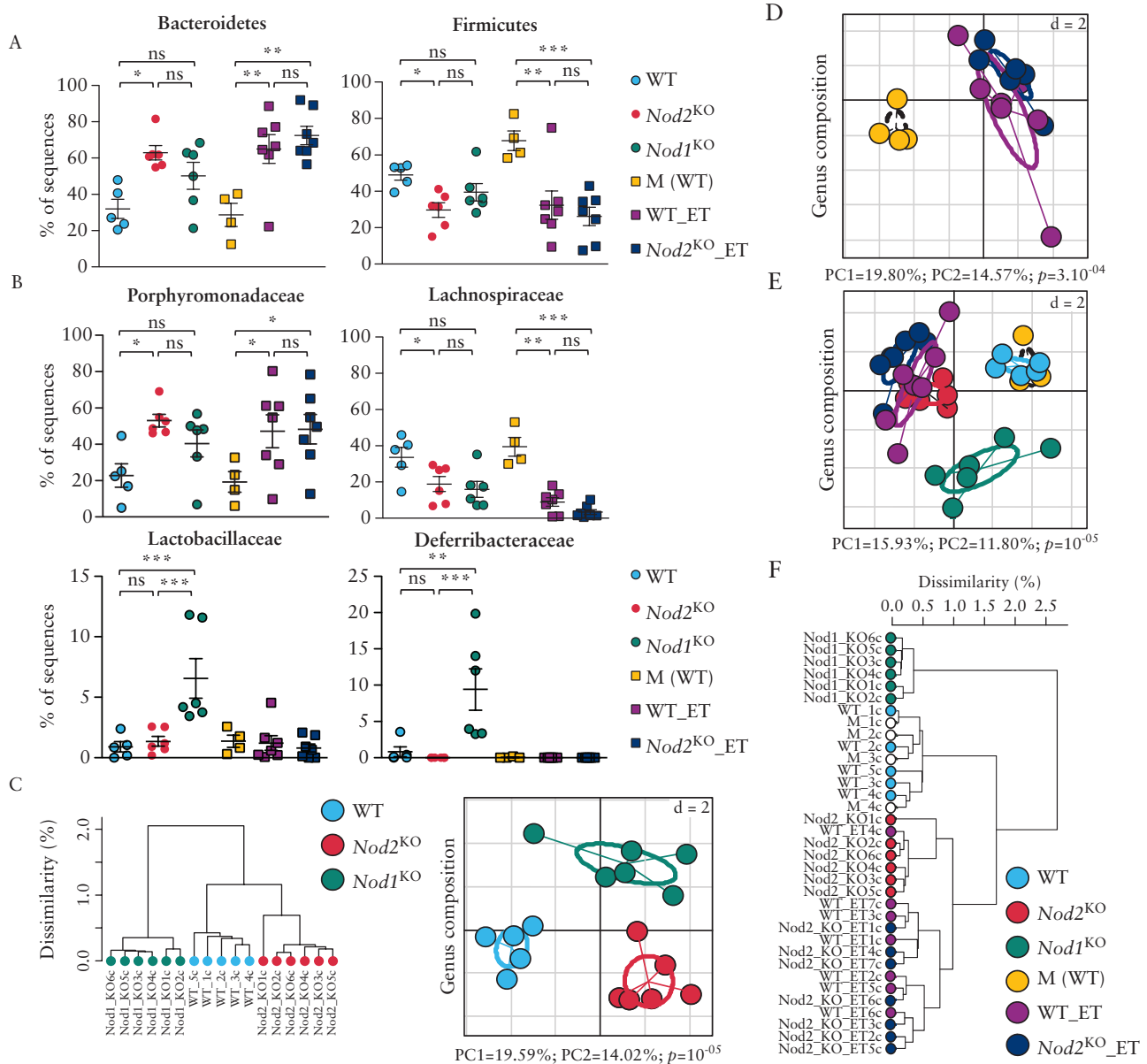


Figure 1. Nod2 deficiency induces specific and dominant bacterial dysbiosis in colon. Proportion of colonic microbiota at phyla [A] and family [B] level in C57BL/6 wild-type [WT], *Nod2*^{KO}, and *Nod2*^{ZKO} mice and mice obtained by embryo transfer [ET]. [C] Principal component analysis and hierarchical clustering based on bacterial composition at genus level, highlighting that colonic microbiota is dependent on genotype. [D] Colonic microbiota from WT_ET and *Nod2*^{ZKO}_ET mice is different from bacterial communities from their mother. Principal component analysis [E] and hierarchical clustering [F] based on genus bacterial composition in WT_ET and *Nod2*^{ZKO}_ET mice clustered with *Nod2*^{ZKO} mice that differ to *Nod1*^{KO} and WT mice. One point indicates one mouse; mean ± standard error of the mean [SEM]; **p* < 0.05, ***p* < 0.01, and ****p* < 0.001 vs indicated groups.

3.2. Nod2 deficiency leads to dominant mucosa-associated microbial dysbiosis

The gut microbiota is in part maternally transmitted, and long-term breeding of isolated mouse colonies may result in marked differences between mouse strains.³⁷ To normalise the microbial colonisation of WT and *Nod2*^{KO} pups, we conducted embryo transfer [ET] experiments. Embryos from *Nod2*^{KO} and WT mice were mixed and transferred to pseudopregnant WT recipient mothers. After birth, littermate pups (referred to as WT_ET and *Nod2*^{KO}_ET) were maintained in the same cage. At 10 weeks of age, ileal and colonic microbial composition of WT_ET and *Nod2*^{KO}_ET pups was similar at both phylum and family levels, but differed significantly from that of

their WT mothers [Figure 1A and B and Supplementary Figure 1A]. WT_ET and *Nod2*^{KO}_ET pups exhibited similar microbial compositions at the phylum [Figure 1A] and family [Figure 1B] levels when compared with *Nod2*^{KO} mice. Moreover, increased percentages of bacterial species like the Gram-negative bacterium cL10-2b-4 [*Barnesiella*] and Gram-negative bacterium cTPY-13 [unclassified Porphyromonadaceae] were observed in the colon of WT_ET and *Nod2*^{KO}_ET mice [Supplementary Figure 2A, available as Supplementary data at *ECO-JCC* online]. These results suggested that co-housing was responsible for equilibration of the microbial flora and also indicated that the microbiota of *Nod2*^{KO} mice was transmissible to WT mice.

3.3. The levels of proteins secreted by the epithelium are correlated with the microbial composition.

To define whether defective secretion of antimicrobial peptides or other proteins by the epithelium might contribute to dysbiosis, gene expression was investigated by quantitative PCR in ileal and colonic biopsies. Expression of RegIII γ , RegIII β , and sPLA2 was decreased in the ileum of *Nod2*^{KO} mice [Figure 2]. Noteworthy, expression of pLys, Ang4, Mmp7, pan-cryptdin marker [Figure 2], CRS1C, cryptdin-1, cryptdin-5, and cryptdin-6 [data not shown] was not altered in *Nod2*^{KO} mice. Trefoil factor 3 [TFF3], Fc-fragment of IgG binding protein [Fc- γ Bp], and Muc4 were expressed at higher levels in ileum and colon of *Nod2*^{KO} mice [Figure 2]. In contrast, ileal and colonic biopsies from *Nod1*^{KO} mice displayed distinct profiles from *Nod2*^{KO} mice, highlighting that antimicrobial peptides and mucins were induced by different pathways [Figure 2]. Gene expression was also determined in the ET model. Expression levels of RegIII γ , RegIII β , sPLA2, TFF3, and Fc- γ Bp in WT_ET and *Nod2*^{KO}_ET mice were similar to those observed in *Nod2*^{KO} mice. However, the gene expression profiles in WT mothers were unchanged [Figure 2]. PCA confirmed that host gene expression was driven not only by the genetic background but also by composition of the gut microbiota [Figure 2].

Moreover, the alteration of gene expression of both antimicrobial peptides and mucins was independent of the number of Paneth and goblet cells in ileal but not in colonic crypts [Supplementary Figures 2C and D, available as Supplementary data at ECCO-JCC online].

To further investigate the possible relationship between gene expression, microbial dysbiosis, and *Nod2* deficiency, we correlated specific bacterial communities and the expression of specific genes in all mouse strains [Supplementary Figure 3, available as Supplementary data at ECCO-JCC online]. The decreased level of ileal RegIII γ mRNA was positively correlated with the proportion of *Barnesiella* irrespective of the genetic background [Figure 3A]. Fc- γ Bp expression was positively correlated with unclassified Lachnospiraceae, whereas a negative correlation was observed between Muc4 expression and the proportions of *Barnesiella* in both ileum and colon [Figure 3].

3.4. *Nod2* specifically controls GALT function independent of gut microbial composition.

Nod2^{KO} mice have enlarged PPs^{22,38} characterised by increased numbers of pro-inflammatory cytokine secreting CD4⁺ T cells.^{22,23,38} Enlarged PPs were observed in *Nod2*^{KO} but not in *Nod1*^{KO} mice, indicating the specificity of GALT alteration. In

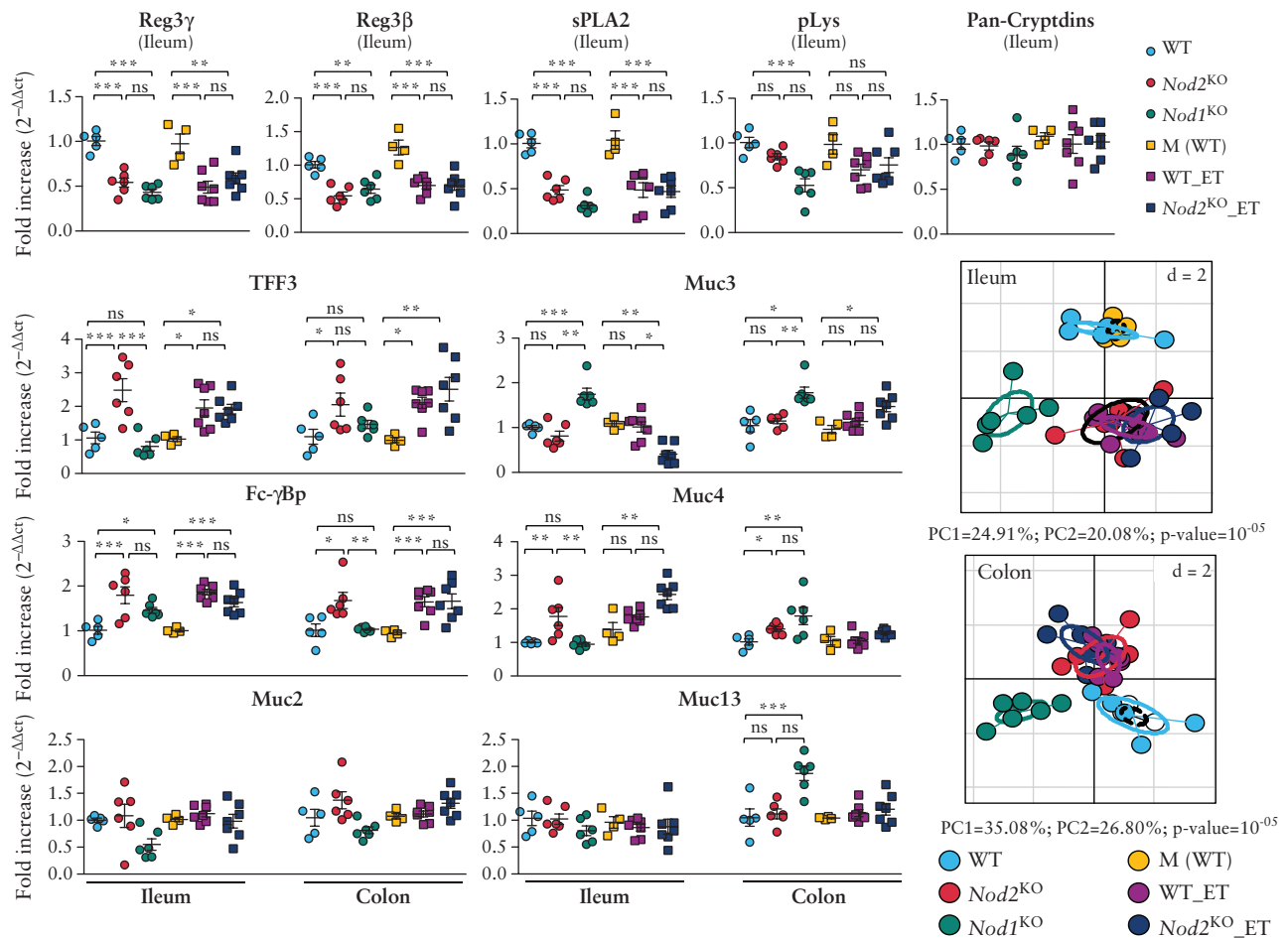


Figure 2. mRNA expression of antimicrobial peptides and mucins. mRNA expression of host genes was measured by quantitative polymerase chain reaction [Q-PCR] in the ileum and colon. Data are expressed in fold-increase using the $2^{-\Delta\Delta C_t}$ method; mean \pm standard error of the mean [SEM]; * $p < 0.05$, ** $p < 0.01$, *** $p < 0.001$ vs indicated groups. Principal component analysis based on mRNA expression in ileum and in colon highlighting that host gene expression is dependent on bacterial composition and genotype. Each data point indicates one mouse.

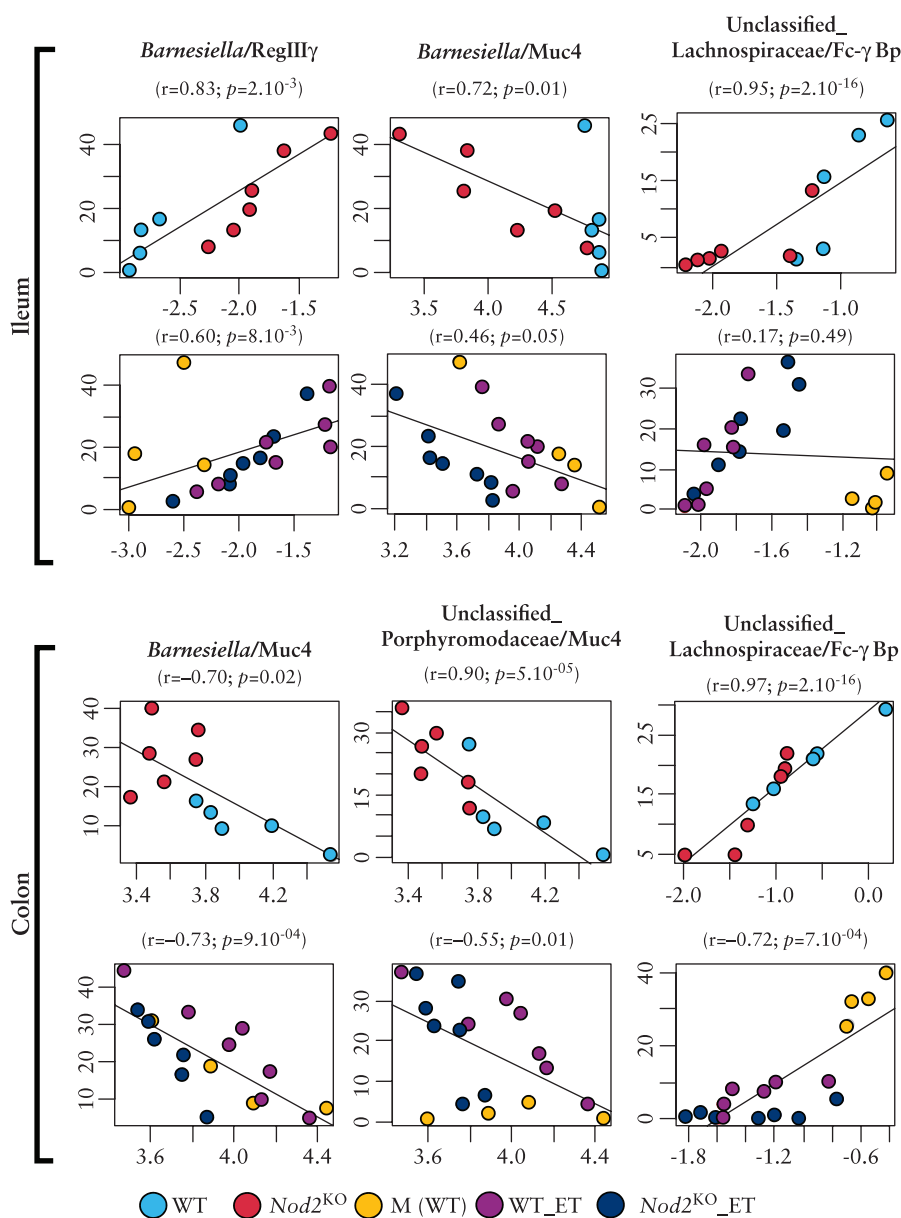


Figure 3. Specific bacteria correlate with antimicrobial peptide and mucin mRNA expression. Spearman correlations between Δ Ct derived from quantitative polymerase chain reaction [qPCR] analyses for host genes and bacterial genera proportions in ileum and colon of wild-type [WT], *Nod2*^{KO}, and WT_embryo transfer [ET], *Nod2*^{KO}_ET and mother [M] mice [$n = 7-9$ per group]. Only recurrent correlations are shown.

addition, *Nod2*^{KO} but not *Nod1*^{KO} mice were characterised by an increase in CD4⁺ T cells and a decrease in CD8⁺ T cells, B cells, and dendritic cells [Figure 4A]. Despite the fact that WT_ET showed bacterial dysbiosis similar to *Nod2*^{KO}_ET mice, PP size and immune cell composition was similar to those observed in WT mice [Figure 4A]. GALT anomalies in *Nod2*^{KO}_ET mice were comparable to *Nod2*^{KO} mice, highlighting that the specific role of Nod2 for regulation of GALT structure is independent of dysbiotic microbiota.

Nod2^{KO} mice are characterised by an increase of intestinal paracellular permeability and bacterial translocation across PP.^{22,23} To investigate whether this phenotype is dependent on *Nod2* deficiency, we compared gut permeability in *Nod1*^{KO} and *Nod2*^{KO} mice. In fact, elevated FITC-dextran levels in serum as well as increased intestinal paracellular permeability in PPs, ileum,

and colon were observed in *Nod2*^{KO} but not in *Nod1*^{KO} mice [Figure 4B]. Furthermore, unlike *Nod1*^{KO} mice, *Nod2*^{KO} mice were more permissive to translocation of *E. coli* K12 across PPs, indicating that only Nod2 is involved in regulation of intestinal barrier function. Moreover, in contrast to WT_ET mice, *Nod2*^{KO} and *Nod2*^{KO}_ET mice exhibited increased paracellular permeability and bacterial translocation [Figure 4B]. These results demonstrate that Nod2 specifically controls epithelial barrier function independently of gut microbiota.

4. Discussion

CD and related *NOD2* mutations have been associated with modifications of gut microbial communities in both humans and mice.^{13,14,15,16,39} We here confirm that *Nod2* deficiency is associated

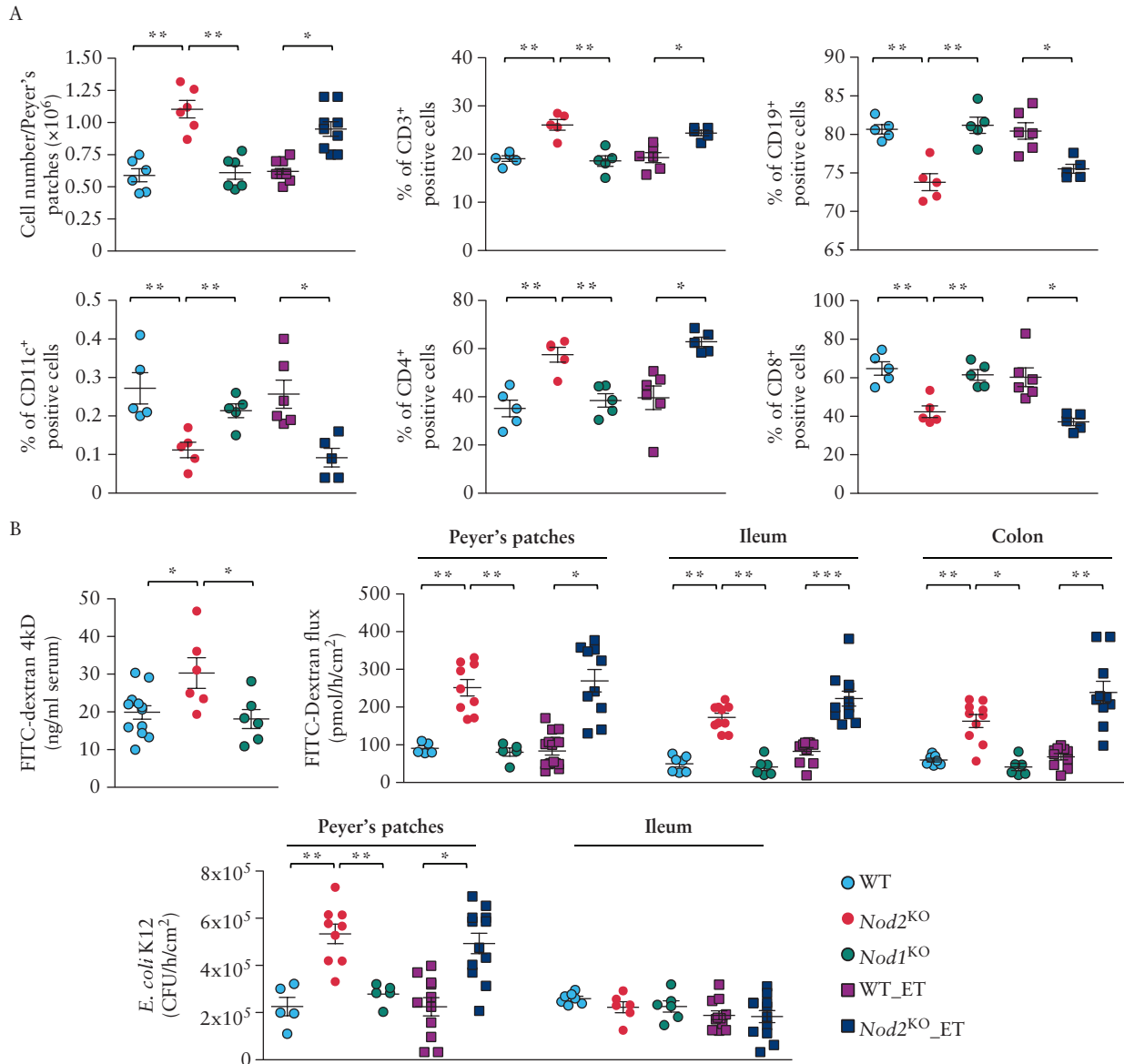


Figure 4. *Nod2* regulates immune cell composition and epithelial permeability in Peyer's patches [PP]. [A] PP cells were counted in a Mallassez cell and the relative number of cells expressing CD3, CD4, CD8, CD19, or CD11c was assessed by flow cytometry. [B] Paracellular permeability and *E. coli* K12 translocation were monitored in serum and by Ussing chambers. Each point indicates one mouse; three independent experiments; mean \pm standard error of the mean [SEM]; * $p < 0.05$, ** $p < 0.01$, *** $p < 0.001$ vs indicated groups.

with intestinal microbial dysbiosis. However, the strong variability of the operational taxonomic units assigned to SFB^{37,40} in the ileum does not allow firm conclusions.

Because a drift of microbiota composition may be seen between animals reared apart, we carefully looked for a 'cage effect', without success [data not shown]. Because a cage effect has been related to *Helicobacter* infections,⁴¹ we also carefully monitored our animal facility but we were not able to detect any infection. On the contrary, the homogeneous data set obtained across all mouse models indicates that *Nod2*-associated microbial dysbiosis is a robust trait. Bacterial dysbiosis in *Nod2*^{KO} mice was particularly characterised by an excess of *Barnesiella* and unclassified Porphyromonadaceae [Bacteroidetes] and a decreased proportion of *Clostridium* XIVa and unclassified Lachnospiraceae [Firmicutes]. These results are in accordance with the changes that were reported in CD patients.

Finally, bacterial dysbiosis is specific to *Nod2* deficiency since it differs from that observed in *Nod1*^{KO} mice.

It has been previously reported that separately elevated *Nod2*^{KO} and WT mice show differences in microbial composition,¹⁶ whereas co-housed WT and *Nod1*^{KO} or *Nod2*^{KO} mice shared the same microbiota^{17,18}. The present data conciliate between these apparently opposite results. *Nod2*^{KO} mice obtained by ET acquired a microbiota different from their WT mothers, confirming the impact of *Nod2* deficiency in the active acquisition of dysbiosis. However, the acquired dysbiosis was transmissible to WT animals, confirming the homogenisation of the gut flora between co-housed mice [likely through coprophagy]. Of note, the transmission of dysbiosis to co-housed WT mice was also reported for *ASC*^{KO}, *NLRP6*^{KO}, and *CD45*^{KO} mice^{42,43}. If confirmed in humans and assuming that the microbiota contributes to CD development, a common dysbiosis

shared by people in close contact could explain the high incidence of CD observed in spouses and the non-random distribution of CD patients within multiplex sibships.⁴⁴

Bacterial dysbiosis in *Nod2*^{KO} mice was accompanied by changes in the secretion of luminal proteins by epithelial cells. A similar link between microbiota and the protein secretion profile was found in all experimental models investigated. In fact, WT mice which acquired bacterial dysbiosis from *Nod2*^{KO} mice by co-housing shared the same gene expression profile. This observation may explain discrepancies in mRNA expression of α -cryptidins^{15,20,45} or RegIII γ ,^{17,18} depending on animal housing conditions. Our results also point out possible feedback loops between host gene expression and specific bacterial components.

NOD2 deficiency in humans and mice is characterised by a gut barrier defect and excessive GALT activation. Accordingly, our animal models showed that alterations of intestinal permeability and GALT were closely linked. The association of an increased gut permeability and abnormality of mucosal lymphocytes was previously reported in *Nod2*^{KO} mice, thereby underlining the intrinsic role of *Nod2* independently of animal housing.⁴⁶ Although bacterial dysbiosis drives neither GALT nor intestinal barrier dysfunctions, antibiotic treatment was sufficient to normalise barrier function and GALT in *Nod2*^{KO} mice.²³ Thus, microbiota is involved in gut mal-function but microbial dysbiosis has no specific impact. Our findings are consistent with the absence of inflammatory markers in WT mice co-housed with *Nod2*^{KO} although both harbour the same grade of dysbiosis.¹³

In conclusion, our results show that microbial dysbiosis associated with *Nod2* deficiency is specific and is transmissible to WT mice. Microbial dysbiosis alters expression of mucins and antimicrobial peptides but has no effect on intestinal permeability or gut-associated lymphoid tissue.

Funding

Financial support was provided by INSERM, labex inflamex, the Université Paris Diderot and the Association François Aupetit.

Conflict of Interest

All authors have no conflict of interest.

Author Contributions

Conceived and designed the experiments: ZAN, JPH, and FB. Performed the experiments: ZAN, PL, PM, NM, MR, KLR, MD, DB, and FB. Analysed the data: ZAN, PL, NM, DB, JPH, and FB. Contributed to the writing of the manuscript: ZAN, PL, DB, JPH, and FB.

Supplementary Data

Supplementary data are available at *ECCO-JCC* online.

References

- Hollander D, Vadheim CM, Brettholz E, Petersen GM, Delahunty T, Rotter JI. Increased intestinal permeability in patients with Crohn's disease and their relatives. A possible etiologic factor. *Ann Intern Med* 1986;105:883–5.
- Horton F, Wright J, Smith L, Hinton PJ, Robertson MD. Increased intestinal permeability to oral chromium [51 Cr]-EDTA in human Type 2 diabetes. *Diabet Med* 2014;31:559–63.
- Hamilton MK, Boudry G, Lemay DG, Raybould HE. Changes in intestinal barrier function and gut microbiota in high-fat diet-fed rats are dynamic and region dependent. *Am J Physiol Gastrointest Liver Physiol* 2015;308:G840–51.
- Barreau F, Hugot J. Intestinal barrier dysfunction triggered by invasive bacteria. *Curr Opin Microbiol* 2014;17C:91–8.
- Nouri M, Bredberg A, Westrom B, Lavasani S. Intestinal barrier dysfunction develops at the onset of experimental autoimmune encephalomyelitis, and can be induced by adoptive transfer of auto-reactive T cells. *PLoS One* 2014;9:e106335.
- Podolsky DK. Inflammatory bowel disease. *N Engl J Med* 2002;347:417–29.
- Hugot JP, Chamaillard M, Zouali H, et al. Association of NOD2 leucine-rich repeat variants with susceptibility to Crohn's disease. *Nature* 2001;411:599–603.
- Girardin SE, Boneca IG, Viala J, et al. Nod2 is a general sensor of peptidoglycan through muramyl dipeptide [MDP] detection. *J Biol Chem* 2003;278:8869–72.
- Philpott DJ, Sorbara MT, Robertson SJ, Croitoru K, Girardin SE. NOD proteins: regulators of inflammation in health and disease. *Nat Rev Immunol* 2014;14:9–23.
- Seksik P, Rigottier-Gois L, Gramet G, et al. Alterations of the dominant faecal bacterial groups in patients with Crohn's disease of the colon. *Gut* 2003;52:237–42.
- Denou E, Lolmede K, Garidou L, et al. Defective NOD2 peptidoglycan sensing promotes diet-induced inflammation, dysbiosis, and insulin resistance. *EMBO Mol Med* 2015;7:259–74.
- Ramanan D, Tang MS, Bowcutt R, Loke P, Cadwell K. Bacterial sensor Nod2 prevents inflammation of the small intestine by restricting the expansion of the commensal *Bacteroides vulgatus*. *Immunity* 2014;41:311–24.
- Couturier-Maillard A, Secher T, Rehman A, et al. NOD2-mediated dysbiosis predisposes mice to transmissible colitis and colorectal cancer. *J Clin Invest* 2013;123:700–11.
- Mondot S, Barreau F, Al Nabhani Z, et al. Altered gut microbiota composition in immune-impaired *Nod2*^{-/-} mice. *Gut* 2012;61:634–5.
- Petnicki-Ocwieja T, Hrnčir T, Liu YJ, et al. Nod2 is required for the regulation of commensal microbiota in the intestine. *Proc Natl Acad Sci U S A* 2009;106:15813–8.
- Rehman A, Sina C, Gavrilova O, et al. Nod2 is essential for temporal development of intestinal microbial communities. *Gut* 2011;60:1354–62.
- Robertson SJ, Zhou JY, Geddes K, et al. Nod1 and Nod2 signaling does not alter the composition of intestinal bacterial communities at homeostasis. *Gut Microbes* 2013;4:222–31.
- Shanahan MT, Carroll IM, Grossniklaus E, et al. Mouse Paneth cell antimicrobial function is independent of Nod2. *Gut* 2014;63:903–10.
- Salzman NH, Hung K, Haribhai D, et al. Enteric defensins are essential regulators of intestinal microbial ecology. *Nat Immunol* 2010;11:76–83.
- Kobayashi KS, Chamaillard M, Ogura Y, et al. Nod2-dependent regulation of innate and adaptive immunity in the intestinal tract. *Science* 2005;307:731–4.
- Jung C, Hugot JP, Barreau F. Peyer's patches: the immune sensors of the intestine. *Int J Inflam* 2010;2010:823710.
- Barreau F, Meinzer U, Chareyre F, et al. CARD15/NOD2 is required for Peyer's patches homeostasis in mice. *PLoS One* 2007;2:e523.
- Barreau F, Madre C, Meinzer U, et al. Nod2 regulates the host response towards microflora by modulating T cell function and epithelial permeability in mouse Peyer's patches. *Gut* 2010;59:207–17.
- Viala J, Chaput C, Boneca IG, et al. Nod1 responds to peptidoglycan delivered by the *Helicobacter pylori* CAG pathogenicity island. *Nat Immunol* 2004;5:1166–74.
- Alnabhani Z, Montcuquet N, Biaggini K, et al. *Pseudomonas fluorescens* alters the intestinal barrier function by modulating IL-1 β expression through hematopoietic NOD2 signaling. *Inflamm Bowel Dis* 2015;21:543–55.
- Johansson ME, Thomsson KA, Hansson GC. Proteomic analyses of the two mucus layers of the colon barrier reveal that their main component, the Muc2 mucin, is strongly bound to the Fcgbp protein. *J Proteome Res* 2009;8:3549–57.

27. Hooper LV, Stappenbeck TS, Hong CV, Gordon JI. Angiogenins: a new class of microbicidal proteins involved in innate immunity. *Nat Immunol* 2003;4:269–73.
28. Bevins CL, Salzman NH. Paneth cells, antimicrobial peptides and maintenance of intestinal homeostasis. *Nat Rev Microbiol* 2011;9:356–68.
29. Salzman NH, Underwood MA, Bevins CL. Paneth cells, defensins, and the commensal microbiota: a hypothesis on intimate interplay at the intestinal mucosa. *Semin Immunol* 2007;19:70–83.
30. Lepage P, Seksik P, Sutren M, et al. Biodiversity of the mucosa-associated microbiota is stable along the distal digestive tract in healthy individuals and patients with IBD. *Inflamm Bowel Dis* 2005;11:473–80.
31. Caporaso JG, Kuczynski J, Stombaugh J, et al. QIIME allows analysis of high-throughput community sequencing data. *Nat Methods* 2010;7:335–6.
32. Li W, Godzik A. Cd-hit: a fast program for clustering and comparing large sets of protein or nucleotide sequences. *Bioinformatics* 2006;22:1658–9.
33. Cole JR, Wang Q, Cardenas E, et al. The Ribosomal Database Project: improved alignments and new tools for rRNA analysis. *Nucleic Acids Res* 2009;37:D141–5.
34. Romesburg HC. Exploring, confirming and randomisation tests. *Comput Geosci* 1985;11:19–37.
35. Meinzer U, Barreau F, Esmiol-Welterlin S, et al. *Yersinia pseudotuberculosis* effector YopJ subverts the Nod2/RICK/TAK1 pathway and activates caspase-1 to induce intestinal barrier dysfunction. *Cell Host Microbe* 2012;11:337–51.
36. Jung C, Meinzer U, Montcuquet N, et al. *Yersinia pseudotuberculosis* disrupts intestinal barrier integrity through haematopoietic TLR-2 signaling. *J Clin Invest* 2012;122:2239–51.
37. Ubeda C, Lipuma L, Gouberne A, et al. Familial transmission rather than defective innate immunity shapes the distinct intestinal microbiota of TLR-deficient mice. *J Exp Med* 2012;209:1445–56.
38. Biswas A, Liu YJ, Hao L, et al. Induction and rescue of Nod2-dependent Th1-driven granulomatous inflammation of the ileum. *Proc Natl Acad Sci U S A* 2010;107:14739–44.
39. Smith RJ, Jeffries TC, Roudnew B, et al. Metagenomic comparison of microbial communities inhabiting confined and unconfined aquifer ecosystems. *Environ Microbiol* 2012;14:240–53.
40. Larsson E, Tremaroli V, Lee YS, et al. Analysis of gut microbial regulation of host gene expression along the length of the gut and regulation of gut microbial ecology through MyD88. *Gut* 2012;61:1124–31.
41. Hildebrand F, Nguyen TL, Brinkman B, et al. Inflammation-associated enterotypes, host genotype, cage and inter-individual effects drive gut microbiota variation in common laboratory mice. *Genome Biol* 2013;14:R4.
42. Elinav E, Strowig T, Kau AL, et al. NLRP6 inflammasome regulates colonic microbial ecology and risk for colitis. *Cell* 2011;145:745–57.
43. Bauer C, Duewell P, Lehr HA, Endres S, Schnurr M. Protective and aggravating effects of Nlrp3 inflammasome activation in IBD models: influence of genetic and environmental factors. *Dig Dis* 2012;30[Suppl 1]:82–90.
44. Hugot JP, Cezard JP, Colombel JF, et al. Clustering of Crohn's disease within affected sibships. *Eur J Hum Genet* 2003;11:179–84.
45. Wehkamp J, Harder J, Weichenthal M, et al. NOD2 [CARD15] mutations in Crohn's disease are associated with diminished mucosal alpha-defensin expression. *Gut* 2004;53:1658–64.
46. Amendola A, Butera A, Sanchez M, Strober W, Boirivant M. Nod2 deficiency is associated with an increased mucosal immunoregulatory response to commensal microorganisms. *Mucosal Immunol* 2012;7:391–404.